USAFETAC/PR-91/002

DTIC FILE COPY

AD-A232 775

MINOT AFB WIND STUDY

by

Major Walter F. Miller

JANUARY 1991

APPROVED FOR PUBLIC RELEASE;
DISTRIBUTION IS UNLIMITED

USAF
ENVIRONMENTAL TECHNICAL
APPLICATIONS CENTER

Scott Air Force Base, Illinois, 62225-5438

REVIEW AND APPROVAL STATEMENT

USAFETAC/PR-91/002, *Minot AFB Wind Study*, January 1991, has been reviewed and is approved for public release. There is no objection to unlimited distribution of this document to the public at large, or by the Defense Technical Information Center (DTIC) to the National Technical Information Service (NTIS).

PATRICK J. BREITLING
Chief Scientist

FOR THE COMMANDER

WALTER S. BURGMANN
Scientific and Technical Information
Program Manager
17 January 1991

REPORT DOCUMENTATION PAGE

2. Report Date: January 1991

3. Report Type: Project Report

4. Title: Minot AFB Wind Study

6. Author: Maj Walter F. Miller

7. Performing Organization Name and Address: USAF Environmental Technical Applications Center (USAFETAC/DNO), Scott AFB, IL 62225-5438

8. Performing Organization Report Number: USAFETAC/PR-91/002

12. Distribution/Availability Statement: Approved for public release; distribution is unlimited.

13. Abstract: This report documents the development and evaluation of 11 algorithms for forecasting gusty northwest winds at Minot AFB, ND. Six of the algorithms used pressure gradients between Dickinson, ND, and Portage la Prairie, Canada, and between Glasgow, MT, and Yorkton, Canada. The other five used the 850 or 700 mb wind over Glasgow, MT. One of the algorithms was found to have skill in forecasting gusty winds and was recommended for operational use.

14. Subject Terms: FORECASTING, WEATHER FORECASTING, WIND, GUSTS, ALGORITHMS, MINOT AFB, NORTH DAKOTA.

15. Number of Pages: 52

17. Security Classification of Report: Unclassified

18. Security Classification of this Page: Unclassified

19. Security Classification of Abstract: Unclassified

20. Limitation of Abstract: UL

Standard Form 298

PREFACE

This study describes the results of USAFETAC Project 900219, "Minot Wind Study." The analyst was Major Walter F. Miller. The original request (from Det 21, 9 WS, Minot AFB, ND--amended by 3 WW/DOO), tasked USAFETAC to develop a correlation wind study to help forecast gusty northwest winds at Minot AFB between October and March. Det 21 wanted to relate pressure gradients between Dickinson, ND, and Portage la Prairie, Canada, and between Glasgow, MT, and Yorkton, Canada, to Minot surface winds (including gusts) for a 6-hour forecast period. In this study, "pressure gradient" is used loosely to refer to the difference in pressure between two stations. This definition is possible here because the distance between the two points remains constant.

Det 21 also asked USAFETAC to examine a relationship between the 700-mb wind speed reported at Glasgow, MT, and the maximum surface wind speed at Minot for a 12-hour forecast period.

Eleven candidate methods were developed and evaluated. One was found to have skill in forecasting gusty winds for Minot AFB from October through March; it is identified and described in this study.

CONTENTS

FIGURES

TABLES

MINOT AFB WIND STUDY

1. INTRODUCTION

1.1 Why the Study? Accurate wind forecasts--particularly of high winds-are vital to aviation. Aviation wind forecasts are issued in two ways: in the terminal aerodrome forecast (TAF), and in weather warnings or meteorological watches. TAFs predict winds for the next 24 hours with a required accuracy of 10 knots. Weather warning criteria are more stringent, requiring specified thresholds, such as 40 knots. A forecast of 40-knot winds in a TAF, for example, is considered a "hit" if the maximum wind recorded is 38 knots; a weather warning, however, requires *exactly* 40 knots or higher to verify. The requirement to forecast weather warning criteria to this degree of accuracy has led to recurring attempts to develop better predictors. This study, for Minot AFB, ND, is such an attempt.

1.2 The Candidate Algorithms. In this study, USAFETAC/DNO evaluated 11 candidate algorithms for forecasting gusty northwest winds at Minot AFB, ND. Six of these algorithms use surface observations that include pressure gradients between Dickinson, ND, and Portage la Prairie, Canada, and between Glasgow, MT, and Yorkton, Canada. The other five use the 850- or 700-mb wind over Glasgow, MT. One of the 11 algorithms was shown to have skill in forecasting gusty winds and is recommended for operational use.

1.3 The Basic Statistical Relationship. The study found that the best statistical relationship between maximum wind speed and observed variables is:

$$FCSTMAX = 87.97 - 0.08\ SLP + 0.76\ MAXWND + 0.64\ GGWMYQV - 2.00\ HRDUM$$

where:

FCSTMAX = Maximum forecast wind speed (kts) that will occur in the next 6 hours.

MAXWND = Current wind gust or speed (kts).

GGWMYQV = Current pressure gradient (pressure difference) between Glasgow, MT, and Yorkton, Canada in millibars.

SLP = Sea level pressure at Minot.

HRDUM = a dummy variable set to 1 when the starting forecast hour is between 21Z and 09Z; otherwise, it has the value of zero.

This equation is valid only when two pressure gradients (one between Dickinson, ND, and Portage la Prairie, Canada--the other between Glasgow, MT, and Yorkton, Canada) are greater than 1 mb. The locations of the four stations used are shown in Figure 1.

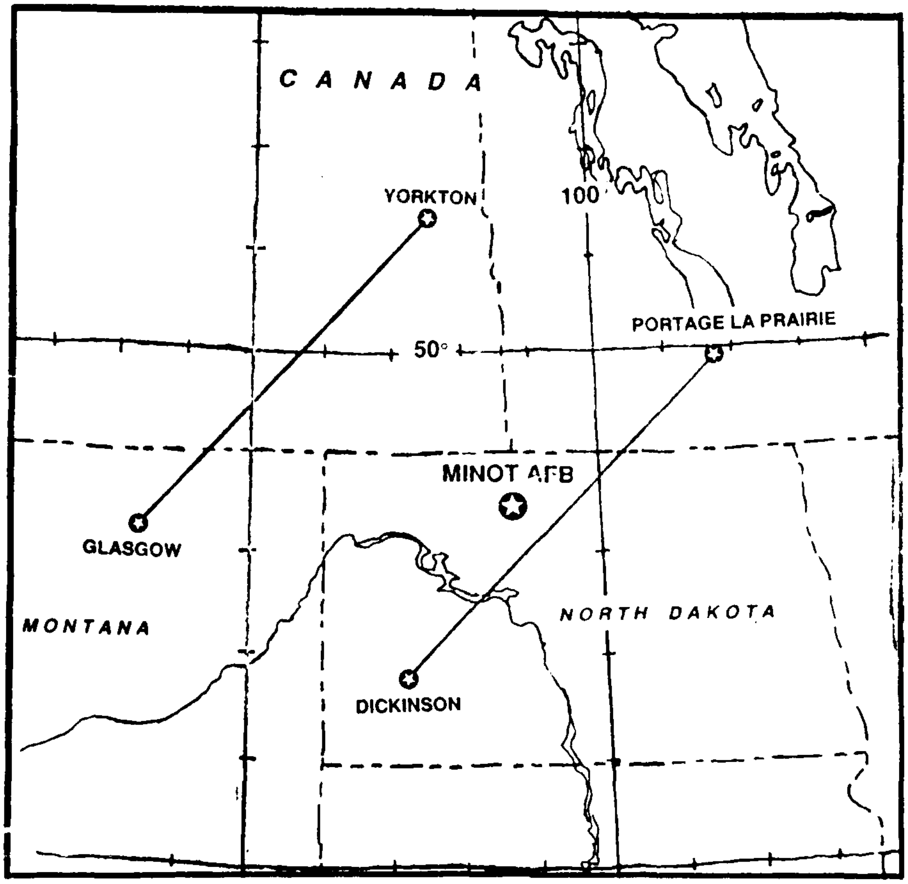

Figure 1. The Four Stations Used for Pressure Gradient Comparisons.

1.4 "Inflated" Wind Speed. When the National Weather Service developed model output statistics (MOS), they defined a procedure called "inflation"--an attempt to improve forecasting high-wind events (Klein, et al., 1959). An "inflated" wind speed can be calculated by:

$$FCSTMAX_i = \frac{FCSTMAX - 19.37}{0.86} + 19.37$$

where $FCSTMAX_i$ is the inflated wind speed and FCSTMAX is the original objective wind speed forecast, both in knots. $FCSTMAX_{ave}$ (19.37 kts) is the mean maximum wind speed for the dependent data set, and R (0.86) is the multiple correlation coefficient from the regression. The inflation procedure increases the wind forecast when it is above the mean, and decreases it when it is below the mean. The use of this procedure is discussed further in Section 3.

1.5 Study Organization. The initial customer request proposed a relationship between the maximum wind and the pressure gradient, based on the geostrophic wind theory discussed in Section 2. The steps for developing and verifying candidate models is discussed in Section 3. Section 4 provides an analysis of the proposed models. A comparison of the MOS wind forecast to our proposed algorithm is provided in Section 5.

2. THEORY

2.1 The Geostrophic Wind Equation. Simplified versions of the equations of motion are used successfully to forecast winds in dynamic models, or manually, by using contour charts. The simplest version is the geostrophic wind equation, given below:

$$u = \frac{-1}{\rho f} \frac{\partial p}{\partial n}$$

where u is the wind component perpendicular to n, and $\frac{\partial p}{\partial n}$ is the derivative of pressure with respect to distance (but which can be approximated as the difference in pressure between two points divided by the distance between the points). The Coriolis parameter is expressed as f, and ρ is the density of the air. The geostrophic wind is derived by assuming: (1) no change in wind velocity with time--a very poor assumption for gusty winds, and (2) the pressure gradient and Coriolis forces are in balance--a good assumption above the boundary layer, but not at the surface.

2.2 Geostrophic Wind Limitations. Attempts to use the geostrophic wind to forecast surface winds are not usually successful. It is the premise of this study that by developing regression coefficients between pressure gradient and maximum wind speed, the errors caused by surface friction, curvature in the pressure pattern, turbulent eddies, and changes in the pressure field with time (especially when making forecasts) can be taken into account. One such statistical relationship (developed for this study) is shown in 1.3.

2.3 Using Upper-Air Data. Upper-air data was used to determine if upper-level winds could be related to maximum surface wind speeds. When the surface is coupled to the upper atmosphere, the winds through the boundary layer are well mixed. This coupling implies that the surface wind speed is related to the winds at 850 or 700 mb. A surface inversion develops at night, and the surface layer becomes decoupled from the atmosphere above. As heating begins in the morning, the surface inversion breaks, allowing upper-level momentum to mix into the surface layer. The peak wind gust for the day may occur before the momentum can be mixed. Success in using upper-air data depends upon knowing when the surface inversion will break. If the ground is covered by snow (or if the sky is overcast) the inversion may remain throughout the day, and the upper-level winds never reach the surface. On a clear day over bare soil, the inversion may break early in the morning, resulting in strong surface winds. If the upper-level momentum is always mixed down to the surface, a statistical relationship might be developed between upper-level and surface winds. Since the inversion is not always broken, other predictands might separate these two cases and improve the maximum wind forecast. Unfortunately, our attempts to develop such a statistical relationship failed.

3. DATA

3.1 Surface observations of sea level pressure, wind speed, wind direction, wind gusts, temperature, sky cover, and ceiling height were obtained from USAFETAC station tapes that contained hourly and special observations from 1973 to 1989 for the five stations listed below. Data from 1973 to 1986 was used as the dependent data set to develop the equations. Data from 1987 through 1989 was used for independent verification of the resulting equations. Only data from October through March was used in developing the algorithm. Winds were converted from meters per second to knots. Temperatures were in degrees Celsius.

STATION	CALL		LAT	LON	ELEV
Minot AFB, ND	MIB	727675	48° 25'N	101° 21'W	508 m
Dickinson, ND	DIK	727645	46° 48'N	102° 48'W	789 m
Glasgow, MT	GGW	727680	48° 13'N	106° 37'W	700 m
Portage la Prairie, Canada	YPG	718510	49° 54'N	98° 16'W	269 m
Yorkton, Canada	YQV	711380	51° 16'N	102° 28'W	498 m

3.2 Upper-level winds at 850 and 700 mb, along with the structure of the inversion and vertical wind shear, were taken from Glasgow, MT, radiosonde observations made from the same location as the Glasgow surface observations. Data was available from 1973 to 1989. Again, the first 14 years were used as the dependent dataset, the last 3 years for independent verification. Winds were converted from metric to English units to be consistent with the surface observations.

4. METHODOLOGY

4.1 Quality Control. First, a gross error check was performed on each variable to quality control the database; only three questionable values were removed. The data was then prepared for linear regression. Some variables could be used directly, but others had to be calculated. Still others were maximum values occurring during the period.

4.1.1 The maximum wind (MAXWND) for each observation is either the value of the gust (when reported) or the wind speed. The maximum wind during the 6-hour period (FCSTMAX) was selected from MAXWND for all observations within that window. FCSTMAX is the dependent or predicted variable throughout this study. The wind direction recorded at the time of the maximum wind during the 6-hour period was kept as MAXPDDIR. A timelag (TIMELAG) was calculated between the the start of the 6-hour period to the time of the maximum wind. This procedure was repeated every 3 hours, beginning at 0000Z.

4.1.2 Because of failure to predict maximum wind in past studies, the mean wind speed (SPDBAR), using hourly observations for the 6-hour forecast period, was calculated. The mean east-west u-component (UDIRBAR) and north-south v-component (VDIRBAR) were also calculated for use in computing the mean wind direction (DIRBAR). The procedures for conversion from wind speed and direction to u- and v-components and vice versa were from AWS/TR-83/001.

4.1.3 After Det 21 told us that high winds normally occur after cold frontal passage, we included sea level pressure (SLP), surface temperature (TEMP), 24-hour change in temperature (DELT24), and sea level pressure (DELP24) at Minot in the study in the hope that these variables would identify conditions following cold front passage.

4.1.4 The sea level pressure differences between Dickinson and Portage La Prairie (DIKMYPG) and between Glasgow and Yorkton (GGWMYQV) were calculated every 3 hours starting at 0000Z. The pressure differences (referred to as "pressure gradients" in this study) are given by

$$\text{DIKMYPG} = \text{SLP}_{\text{DIK}} - \text{SLP}_{\text{YPG}}$$

and

$$\text{GWMYQV} = \text{SLP}_{\text{GGW}} - \text{SLP}_{\text{YQV}}.$$

where SLP is sea level pressure, and the subscripts are weather station call letters (DIK--Dickinson, YPG--Portage la Prairie, GGW--Glasgow, YQV--Yorkton).

4.2 Database Preparation. The database for the regression using upper-air data was prepared in the same way. The steps shown in 4.1 were repeated for a 12-hour period beginning at 00 and 12Z. The surface data was then matched to the upper-air observation at the start time. Upper-air data consisted of wind speed, wind direction, and u- and v-components for 850, 700, and 500 mb. The temperature, pressure, height, and dew point at the top and bottom of the first inversion below 1700 meters MSL, along with the temperature difference between the top and bottom of the inversion, were included in an attempt to determine when the surface inversion would break and allow the mixing of upper-level winds. Wind shear and speed and direction from surface to 850 and 700 mb (to identify post-frontal conditions) were also considered. The variables and their descriptions are given in Table 1.

TABLE 1. Upper-Air Variables Used in the Regression Study.

VARIABLE	DESCRIPTION
WND850	850-mb wind speed in knots
DIR850	850-mb wind direction in degrees
UCOMP85	u-component (E-W) of the 850-mb wind speed in knots
VCOMP85	v-component (N-S) of the 850-mb wind speed in knots
TEMP85	850-mb temperature in Celsius
SPD1085	Magnitude of the shear vector between the surface and 850 mb in knots
DIR1085	Direction of the shear vector between the surface and 850 mb in knots
WND700	700-mb wind speed in knots
DIR700	700-mb wind direction in degrees
UCOMP70	u-component (E-W) of the 700-mb wind speed in knots
VCOMP70	v-component (N-S) of the 700-mb wind speed in knots
TEMP70	700-mb temperature in Celsius
SPD1070	Magnitude of the shear vector between the surface and 700 mb in knots
DIR1070	Direction of the shear vector between the surface and 700 mb in knots
WND500	500-mb wind speed in knots
DIR500	500-mb wind direction in degrees
UCOMP50	u-component (E-W) of the 500-mb wind speed in knots
VCOMP50	v-component (N-S) of the 500-mb wind speed in knots
TEMP50	500-mb temperature in Celsius
INVDEPTH	Depth of the first inversion above the surface and below 700 mb.
STRENGTH	Gradient of temperature across the inversion (C/m).
STABLE	Attempt to determine the stability by subtracting the 850-mb temperature from surface temperature.

4.3 The Pearson Product-Moment Correlation Coefficient (R) was used to identify relationships between variables. The correlation coefficient provides an indication of how closely two variables are related. A positive value indicates a positive relationship, with 1 a perfect match. A negative value indicates a negative relationship, with -1 a perfect match. The square of the correlation coefficient shows that proportion of the total variability in the dependent variable that can be accounted for by the independent variable (Ott, 1988). Table 2 gives an example of the correlation coefficient for the dependent data set when both pressure gradients are greater than 4 mb.

TABLE 2. The Pearson Product-Moment Correlation Coefficient Between the Dependent and Independent Variables--Both Pressure Gradients Greater than 4 mb.

	FCSTMAX	MAXPDDIR	SPDBAR	UDIRBAR	VDIRBAR	DIRBAR
MAXWND	0.817	0.407	0.816	0.681	-0.671	0.478
WNDDIR	0.336	0.749	0.347	0.119	-0.718	-0.796
HR	0.193	0.053	0.155	0.148	-0.090	0.066
TEMPM24	-0.072	0.047	-0.197	-0.266	0.026	0.030
SLPM24	-0.054	-0.157	-0.015	0.063	0.164	-0.169
SLP	-0.167	0.022	-0.108	-0.102	0.019	0.027
TEMP	-0.173	-0.112	-0.289	-0.277	0.217	-0.145
SKY	-0.283	-0.257	-0.262	-0.125	0.321	-0.290
CIGHGT	-0.262	-0.313	-0.249	-0.083	0.366	-0.354
DELT24	-0.064	-0.196	-0.063	0.042	0.217	-0.211
DELP24	-0.091	0.172	-0.079	-0.150	-0.141	0.186
GGWMYQV	0.499	0.108	0.519	0.546	-0.309	0.148
DIKMYPG	0.517	-0.011	0.538	0.654	-0.146	0.004

4.4 FCSTMAX Correlation. As Table 2 indicates, the best FCSTMAX correlation is with the current wind speed (MAXWND). There is also good correlation between the two pressure gradients (GGWMYQV and DIKMYPG) and FCSTMAX. Other variables, such as DELT24 and DELP24, have poor correlations. A better understanding of the correlation coefficients is obtained by using the scatter diagrams in Figures 2 through 6. Figure 2 shows the relationship between FCSTMAX and MAXWND. Since MAXWND is used in the calculation of FCSTMAX, there are no values of FCSTMAX less than MAXWND. Figures 3 and 4 show FCSTMAX as a function of each pressure gradient, but there is a lot of spread in the data; for a pressure gradient (DIKMYPG) of 8 mb, FCSTMAX ranges between 11 and 51 knots. Figures 5 and 6 show the relationship between FCSTMAX and SLP and DELP24, respectively. These are examples of decreasing correlation and the earlier linear pattern becomes just a grouping of points.

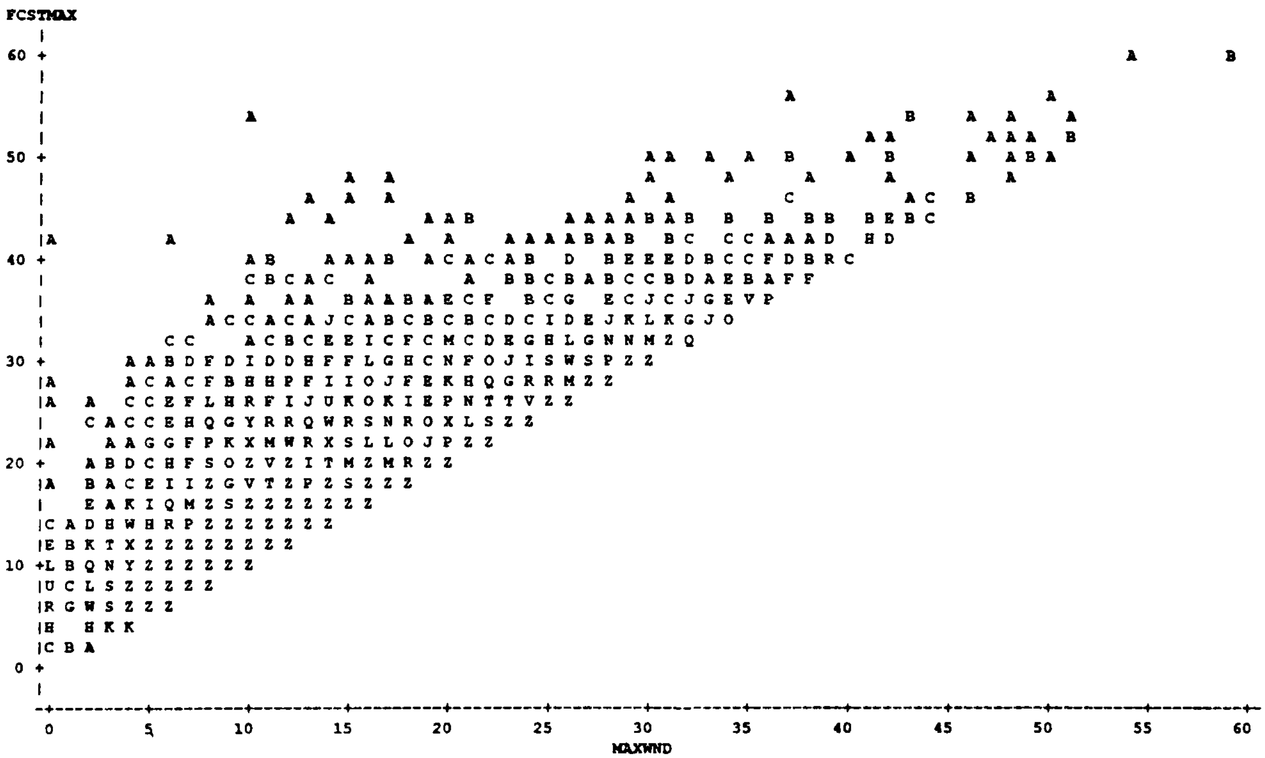

Figure 2. Scatter Diagram of FCSTMAX as a Function of MAXWND--Both Pressure Gradients Greater than 4 mb. A = 1 observation, B = 2 observations, etc.

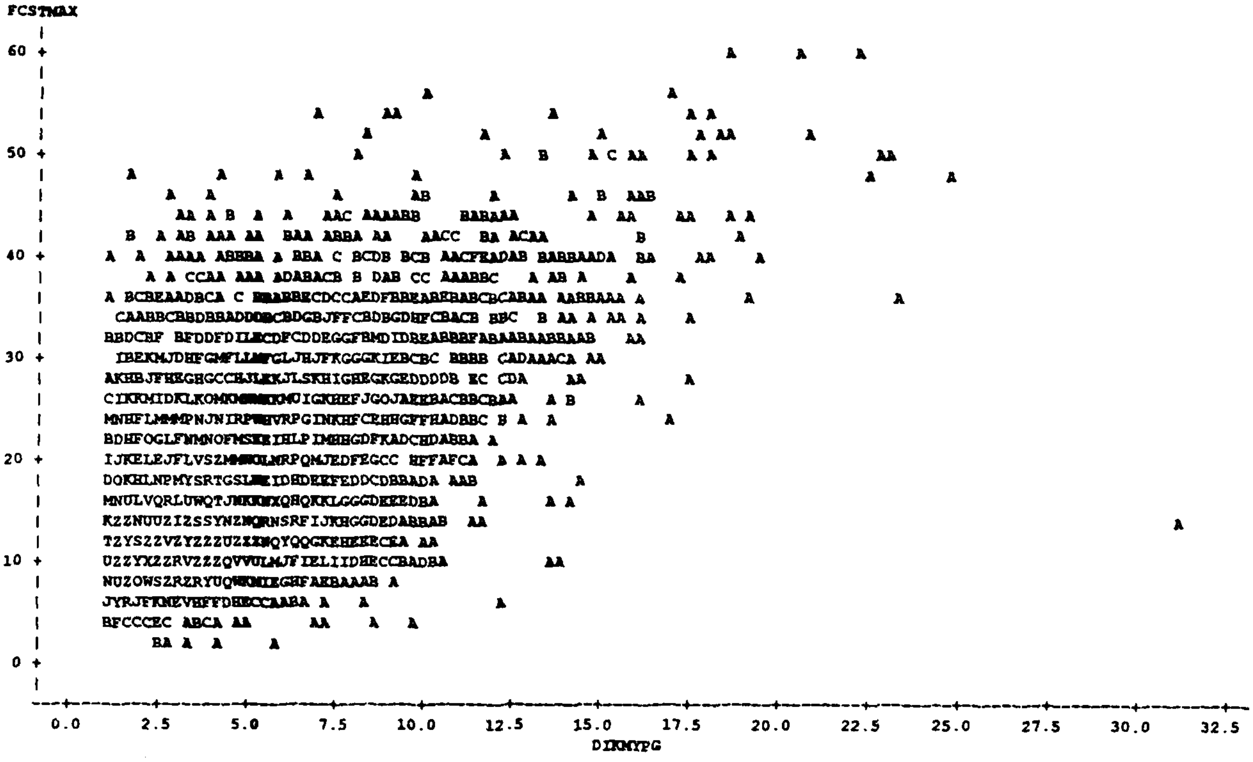

Figure 3. Scatter Diagram of FCSTMAX as a Function of DIKMYPG--Both Pressure Gradients Greater than 4 mb. A = 1 observation, B = 2 observations, etc.

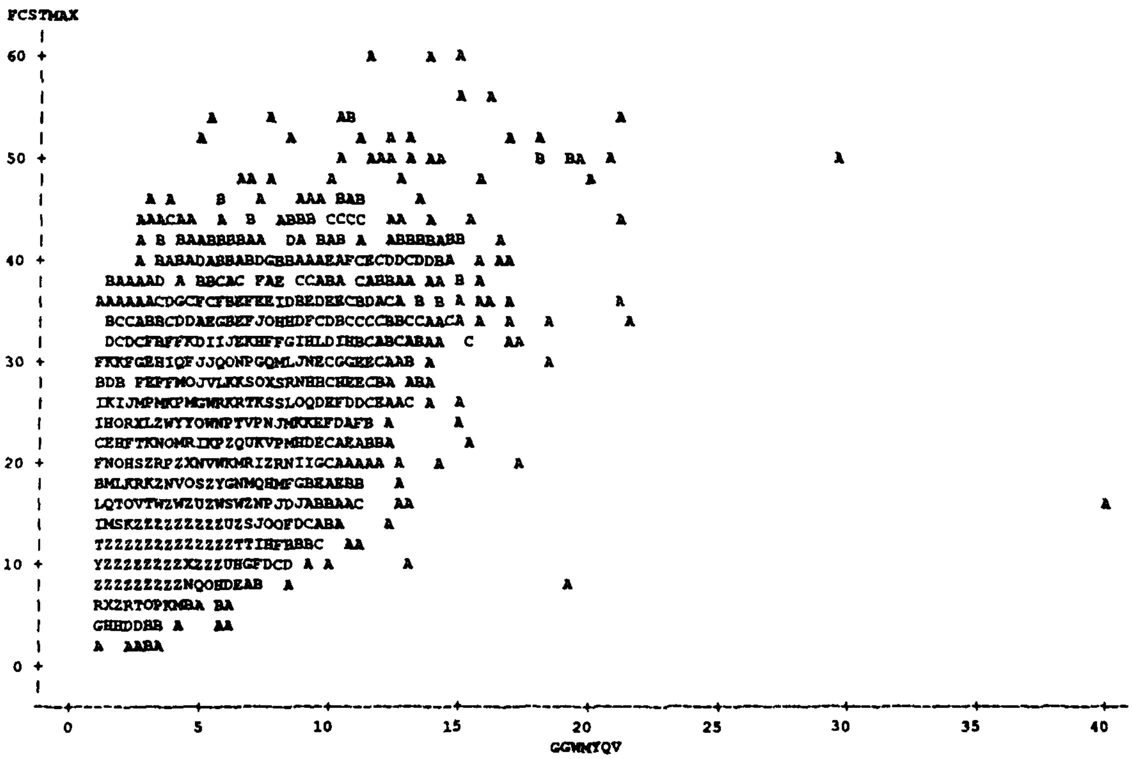

Figure 4. Scatter Diagram of FCSTMAX as a Function of GGWMYQV--Both Pressure Gradients Greater than 4 mb. A = 1 observation, B = 2 observations, etc.

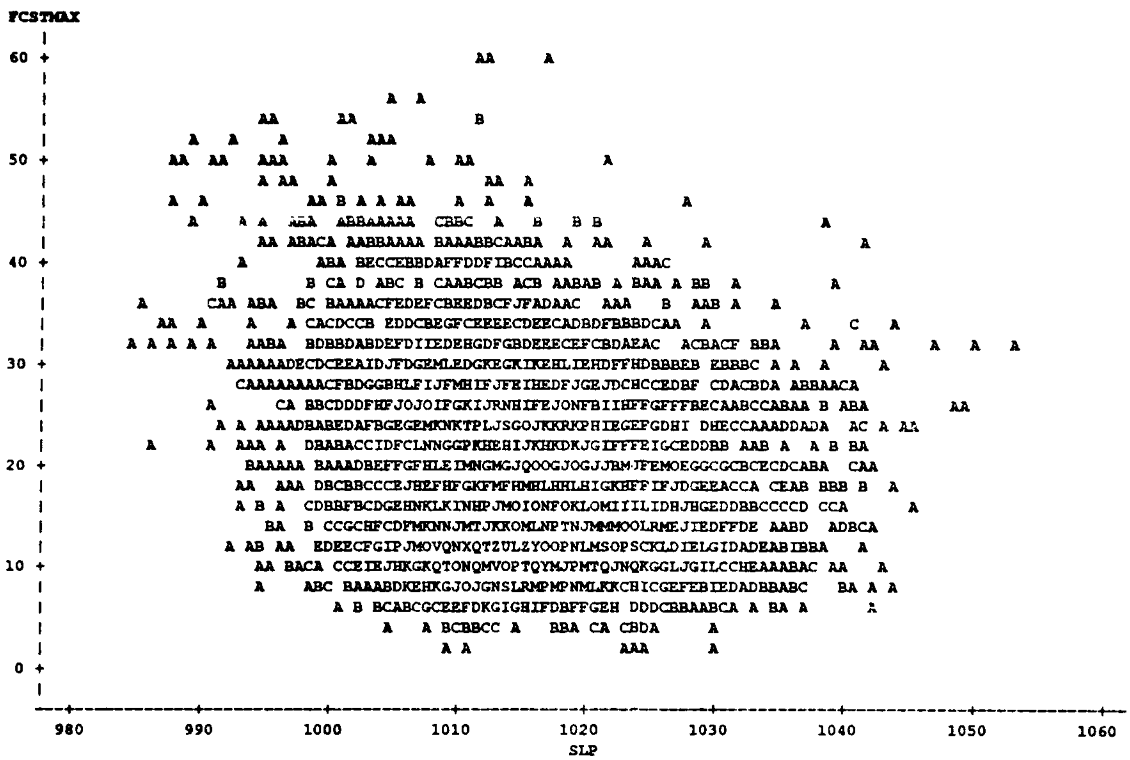

Figure 5. Scatter Diagram of FCSTMAX as a Function of SLP--Both Pressure Gradients Greater than 4 mb. A = 1 observation, B = 2 observations.

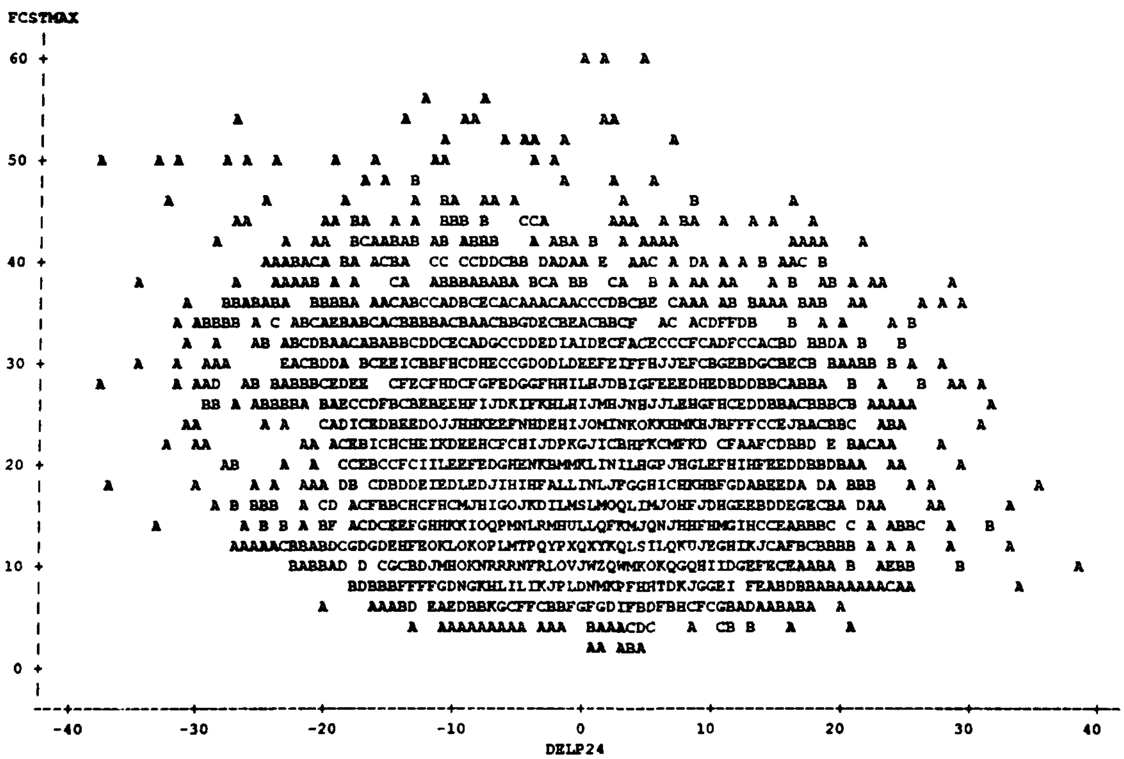

Figure 6. Scatter Diagram of FCSTMAX as a Function of DELP24--Both Pressure Gradients Greater than 4 mb. A = 1 observation, B = 2 observations.

4.5 Model Development from Surface Data. The first regression model (A, in Table 3) is the relationship between FCSTMAX and the two pressure gradients (DIKMYPG and GGWMYQV) proposed by Det 21. When separate linear regressions were run for each 3-hour period of the day, the only difference in the resulting equation was in the y-intercept. To simplify the resulting model to one equation, a dummy variable (HRDUM) was created and set to 1 if the time was between 21 and 09Z; otherwise, it had the value of zero. Models B and C consist of a single pressure gradient (DIKMYPG and GGWMYQV, respectively) as the independent variable for forecasting FCSTMAX. Additional models were developed based on the correlation coefficients shown in Table 2, using the following variables: MAXWND, WNDDIR, SLP, TEMP, DELT24, DELP24, CIGHGT, DIKMYPG, and GGWMYQV. The most significant variable was MAXWND, followed by GGWMYQV. These two, in combination with HRDUM, are shown as model D in Table 3. The third variable identified was SLP; it is included as model E in equation 1. Model F uses all six significant variables; the rest are not statistically significant. Since the correlation coefficient between the independent variables and dependent variables MAXPDDIR, SPDBAR, UDIRBAR, VDIRBAR, and DIRBAR are similar to or less than FCSTMAX, none of these relationships was pursued.

TABLE 3. Candidate Models Using Surface Observations.

MODEL	EQUATION
A	FCSTMAX = 10.27 + 0.81 GGWMYQV + 1.17 DIKMYPG - 2.45 HRDUM
B	FCSTMAX = 10.15 + 1.72 DIKMYPG
C	FCSTMAX = 11.32 + 1.53 GGWMYQV
D	FCSTMAX = 5.75 + 0.77 MAXWND + 0.69 GGWMYQV - 1.90 HRDUM
E	FCSTMAX = 87.97 - 0.08 SLP + 0.76 MAXWND + 0.64 GGWMYQV - 2.00 HRDUM
F	FCSTMAX = 120.90 - 0.11 SLP - 0.09 TEMP + 0.74 MAXWND - 0.05 DELP24 - 0.07 DELT24 + 0.66 GGWMYQV - 1.92 HRDUM

4.6 Candidate Model Evaluation. The candidate models in Table 3 were evaluated using the following indicators (see discussion in Section 5). These statistics were applied to category forecasts of 10-knot increments (0 to 9, 10 to 19, etc.), as well as to a weather warning criterion of 40 knots.

4.6.1 The Coefficient of Determination (R^2) is that proportion of the variability in the dependent variable that is accounted for by the independent variables of the model. R^2 ranges between 0 and 1, with 1 indicating total agreement between the dependent and independent variable. Zero indicates that the variables are unrelated.

4.6.2 The Heidke Skill Score (HSS) is used as defined in AWS TR 235, pp 43-47. The HSS, which ranges from 0 to 1, measures the accuracy of a given forecast method over climatological chance. In the HSS, 1 indicates perfect skill; zero, no skill.

4.6.3 The Probability of Detection (POD) is the ratio of the number of events successfully forecast for a given category to the total number of events that occurred (Goldsmith, 1989). Again, the values range from 0 to 1, with 1 being a perfect forecast.

4.6.4 The False Alarm Rate (FAR) is the ratio of the number of times an event is forecast to happen, but didn't, to the total number of times the event is forecast (Goldsmith, 1989). The lower the FAR, the better--0 is perfect.

4.6.5 The Critical Success Index (CSI) is the ratio of the number of events that are successfully forecast to the sum of the hit, missed opportunities, and false alarms for that category (Goldsmith, 1989). Again, values range from 0 to 1, with 1 a perfect forecast. The advantage of the CSI is that it examines only significant events, and does not take into account how many times good weather is forecast.

4.7 Frequency Distribution. Det 21 wanted the equation to be developed only when both pressure gradients were greater than 4 mb. Because that threshold might miss weather warning events, a frequency distribution was calculated for FCSTMAX for those observations that met the threshold as well as for those observations that had northwest winds (270-360°) greater than 10 knots but did not meet the threshold. A frequency distribution of wind direction when the threshold is met was used to check if a northwest wind direction is a correct forecast.

4.8 The NWS "Inflation Technique." In developing their objective forecast methods, the National Weather Service has had problems in forecasting extreme events. Klein, et al. (1959) developed an "inflation" technique to apply to regression forecasts. The initial objective forecast (S_o) is adjusted by the equation:

$$S_i = \frac{S_o - S_{ave}}{R} + S_{ave}$$

where S_{ave} is the mean of the variable in the dependent dataset and R is the multiple correlation coefficient. We applied this technique to the six candidate models given in Table 2.

4.9 "Inflation" Methodology Applied to Upper-Air Data. The same inflation methodology was used on the upper-air data Det 21 requested. The original request specified 700-mb winds, but 850- and 500-mb winds were included in the correlations to determine which level produced better results. An attempt was made to determine if the surface layer was decoupled from the upper levels by including the strength of the inversion (temperature change per distance) and wind shear between surface and 850 mb and between surface and 700 mb in the study. All these values are correlated with the maximum wind observed during the 12 hours following the sounding observation.

4.10 Correlation Coefficients for Upper-Air Variables. Table 4 gives the correlation coefficients between the upper-air variables and FCSTMAX, MAXPDDIR, SPDBAR, UDIRBAR, VDIRBAR, and DIRBAR. The definition of these variables remains the same as before, but for a 12-hour period instead of 6. These coefficients are valid when the winds are above 30 knots at 850 mb. The best correlations with FCSTMAX are the 850- and 700-mb wind speeds. Figures 10 through 14 show plots of FCSTMAX against WND700, WND850, STABLE, and STRENGTH. WND850, WND700, DIR850, UCOMP85, VCOMP85, SPD1085, DIR1085, STRENGTH, INVDEPTH, and STABLE are used to determine which combinations of variables produce the best regression model

TABLE 4. Pearson Product-Moment Correlation Coefficient for Upper-Air Variables--850-mb Wind Speed Greater than 30 kts, Wind Direction Between 240 and 360°.

	FCSTMAX	MAXPDDIR	SPDBAR	UDIRBAR	VDIRBAR	DIRBAR
WND850	0.511	0.201	0.477	0.403	-0.171	0.216
DIR850	0.202	0.357	0.190	0.419	-0.152	0.360
UCOMP85	0.282	0.281	0.231	0.460	0.078	0.277
VCOMP85	-0.398	-0.426	-0.399	0.565	0.615	-0.441
TEMP85	-0.076	-0.143	-0.164	-0.165	0.371	-0.161
SPD1085	0.256	0.009	0.228	0.128	0.182	0.009
DIR1085	0.066	0.139	0.042	0.210	0.080	0.122
INVDEPTH	-0.055	-0.060	-0.036	-0.080	0.187	-0.074
STRENGTH	-0.016	-0.064	-0.032	.0.069	0.147	-0.049
STABLE	0.138	0.233	0.145	0.308	-0.346	0.240
WND700	0.393	0.209	0.364	0.358	-0.187	0.236

TABLE 4, Cont'd.

	FCSTMAX	MAXPDDIR	SPDBAR	UDIRBAR	VDIRBAR	DIRBAR
DIR700	0.115	0.223	0.107	0.283	-0.098	0.239
UCOMP70	0.226	0.137	0.182	0.258	0.087	0.143
VCOMP70	-0.296	-0.355	-0.309	-0.469	0.462	-0.390
TEMP70	-0.093	-0.205	-0.159	-0.242	0.394	-0.222
SPD1070	0.137	-0.064	0.116	-0.024	0.149	-0.060
DIR1070	0.008	0.044	-0.006	0.117	0.088	0.064
WND500	0.250	0.157	0.223	0.255	-0.138	0.184
DIR500	0.056	0.092	0.040	0.149	-0.012	0.107
UCOMP50	0.171	0.044	0.135	0.128	0.023	0.057
VCOMP50	0.024	-0.109	-0.117	-0.307	0.207	-0.264
TEMP50	-0.091	-0.178	-0.145	-0.211	0.345	-0.186

4.11 Candidate Models Using Upper-Air Data. Candidate models that use upper-air data are listed in Table 5. They include Model U (the customer-proposed relationship between 700-mb winds and FCSTMAX) and Model V, which uses WND850 as the independent variable. Models W and X add a stability variable (STABLE) to the 700- and 850-mb winds. STABLE is the surface temperature minus the 850-mb temperature. The final model (Y) includes WND850 and SHR1085. Separate models are developed for 00 and 12Z because of the large difference in regression coefficients. For models U and W, the 700-mb wind speed is greater than 30 knots and the 700-mb wind direction is greater than 240°. Likewise, the same restrictions are placed on the 850-mb wind speed and direction for models V, X, and Y. All models using upper-air data had coefficients of determination much lower than the surface models. Except for verifying them in the same way as the surface models, no extra effort was spent trying to improve the upper-air models.

TABLE 5. Candidate Models Using Upper-Air Data--Wind Speed Greater than 30 kts, Wind Direction Between 240 and 360°.

U	0000Z	FCSTMAX = 3.77 + 0.38 WND700
	1200Z	FCSTMAX = 6.25 + 0.37 WND700
V	0000Z	FCSTMAX = 7.03 + 0.44 WND850
	1200Z	FCSTMAX = 11.78 + 0.35 WND850
W	0000Z	FCSTMAX = 4.99 + 0.41 WND700 + 0.35 STABLE
	1200Z	FCSTMAX = 11.92 + 0.35 WND700 + 0.53 STABLE
X	0000Z	FCSTMAX = 7.98 + 0.49 WND850 + 0.47 STABLE
	1200Z	FCSTMAX = 14.40 + 0.40 WND850 + 0.61 STABLE
Y	0000Z	FCSTMAX = 5.95 + 0.83 WND850 - 0.52 SPD1085
	1200Z	FCSTMAX = 11.93 + 0.84 WND850 - 0.60 SPD1085

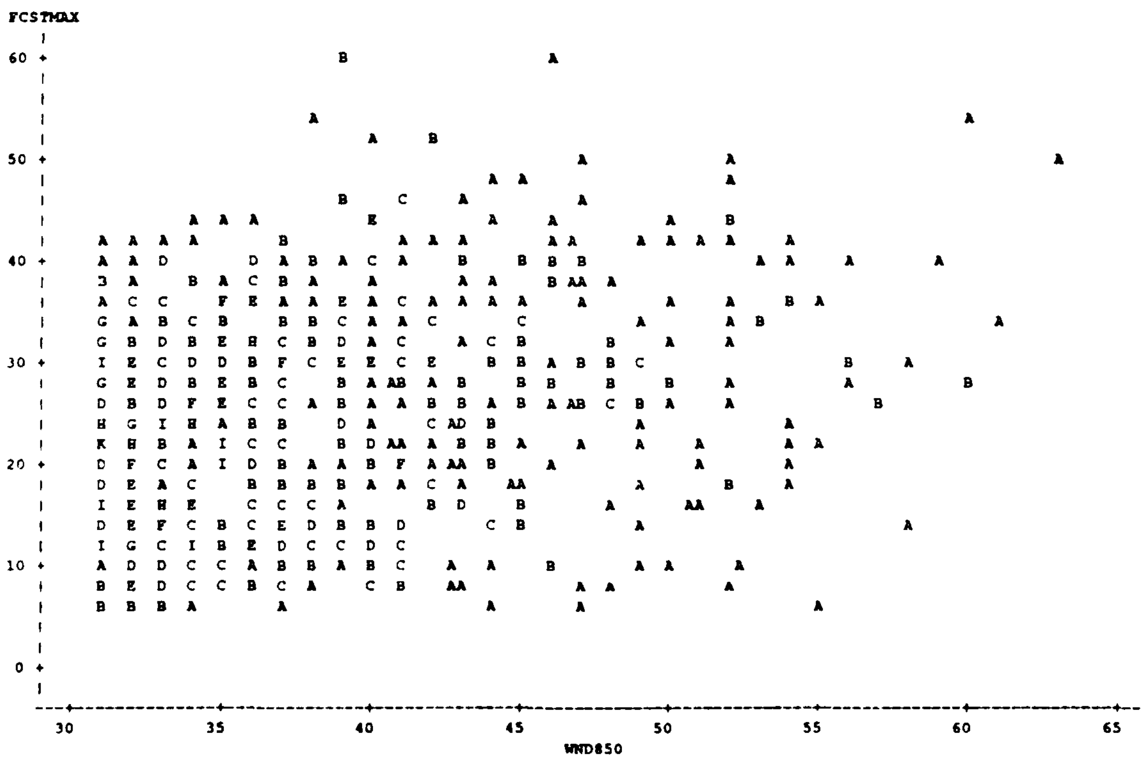

Figure 7. Scatter Diagram of FCSTMAX (12 Hours) as a Function of WND850--WND850 Greater than 30 Knots, Wind Direction Between 240 and 360°. A = 1 observation, B = 2 observations.

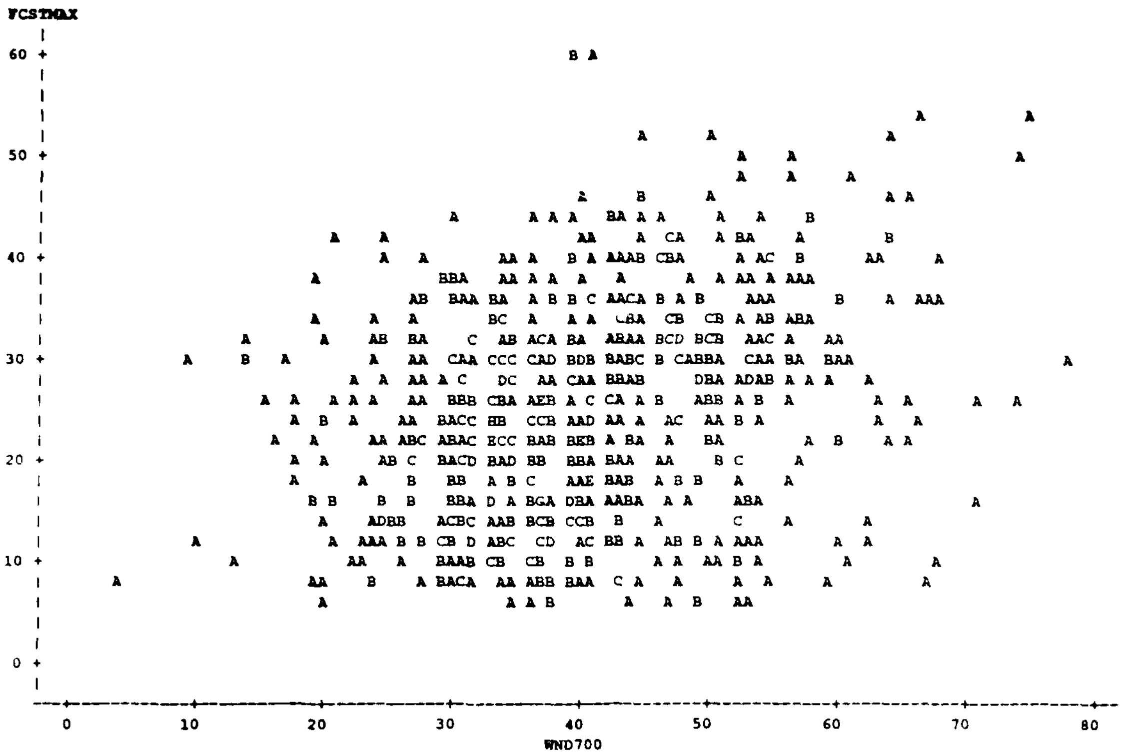

Figure 8. Scatter Diagram of FCSTMAX (12 Hours) as a Function of WND700--WND850 Greater than 30 Knots, Wind Direction Between 240 and 360°. A = 1 observation, B = 2 observations.

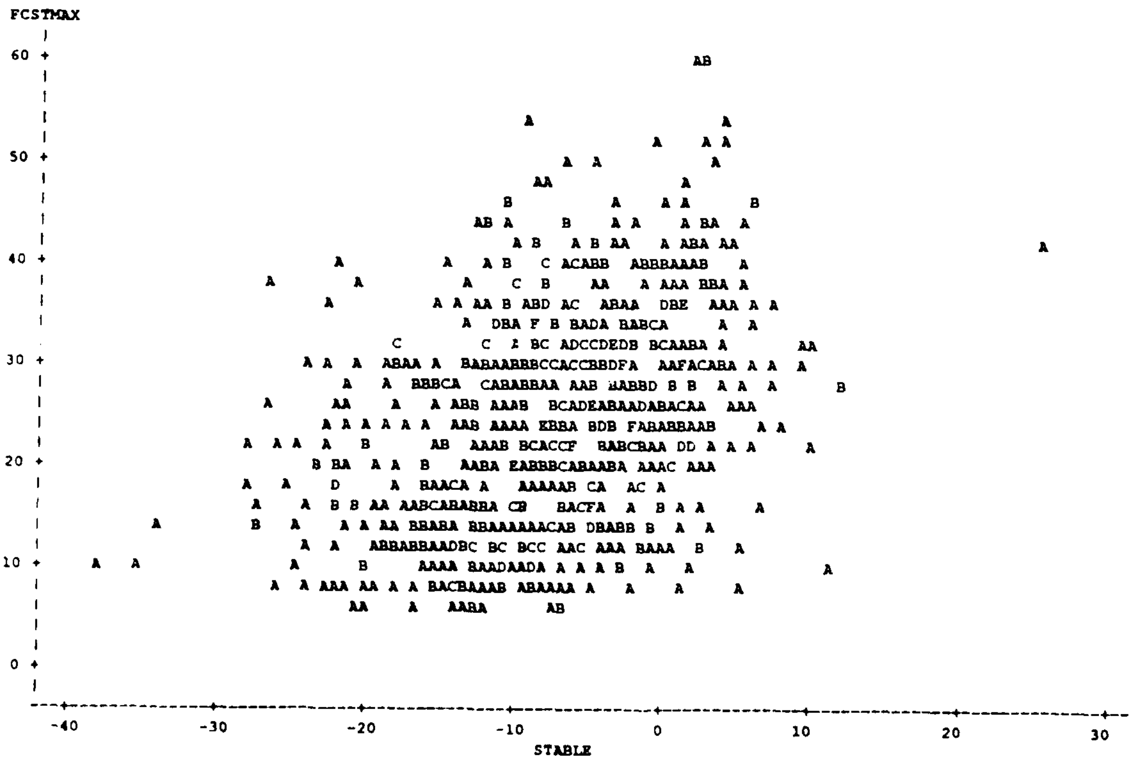

Figure 9. Scatter Diagram of FCSTMAX (12 Hours) as a Function of STABLE--WND850 Greater than 30 Knots, Wind Direction Between 240 and 360°. A = 1 observation, B = 2 observations.

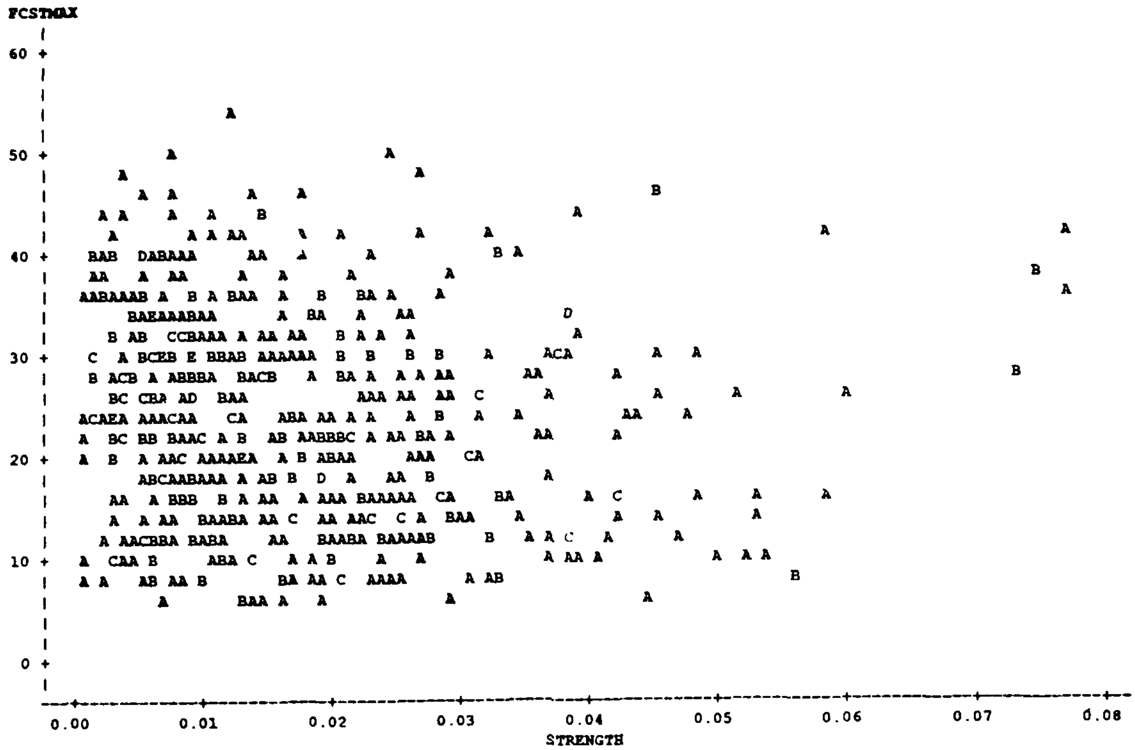

Figure 10. Scatter Diagram of FCSTMAX (12 Hours) as a Function of STRENGTH--WND850 Greater than 30 Knots, Wind Direction Between 240 and 360°. A = 1 observation, B = 2 observations.

5. ANALYSIS, RESULTS, AND VERIFICATION

5.1 Initial Evaluation. Every candidate model was initially evaluated on the dependent data set (73-86) when both pressure gradients were greater than 4 mb. Sample forecast verification matrices for models A and E are provided in Tables 6 and 7. The diagonal from top left to bottom right represents a correct forecast. The percent correct is 47 for model A and 65 for model E. The results for the other models are given in Table 8. Two HSSs are calculated; the first by grouping the wind data every 10 knots, the second by using 40 knots as warning criteria and only consisting of two bins (over and under). Table 8 shows CSI, POD, and FAR calculated for a 40-knot weather warning criterion.

TABLE 6. Verification Matrix for Candidate Model A--Both Pressure Gradients Greater than 4 mb (Dependent Data Set).

OBSVD WINDS	FORECAST WINDS						
	0-9	10-19	20-29	30-39	40-49	50-59	60-69
0-9	0	69	24	1	0	0	0
10-19	0	395	428	9	0	0	0
20-29	0	239	686	58	0	0	0
30-39	0	69	339	129	16	1	0
40-49	0	4	35	45	11	4	0
50-59	0	0	4	7	7	0	0
60-69	0	0	0	0	1	0	0

TABLE 7. Verification Matrix for Candidate Model E--Both Pressure Gradients Greater than 4 mb (Dependent Data Set).

	FORECAST WINDS						
OBSVD WINDS	0-9	10-19	20-29	30-39	40-49	50-59	60-69
0-9	13	80	1	0	0	0	0
10-19	13	650	168	0	0	0	0
20-29	0	246	654	80	0	0	0
30-39	0	33	192	299	28	0	0
40-49	0	0	11	36	47	4	0
50-59	0	1	0	0	8	8	0
60-69	0	0	0	0	0	0	1

TABLE 8. Verification Statistics for Candidate Models Using Surface Observations--Both Pressure Gradients Greater than 4 mb (Dependent Data Set).

Model	**A**	**B**	**C**	**D**	**E**	**F**
R^2	0.344	0.249	0.268	0.722	0.724	0.733
Ten knots						
Percent Correct	47	43	45	65	65	65
HSS	0.316	0.230	0.258	0.620	0.618	0.622
Weather Warning						
Percent Correct	95.7	95.9	95.5	97.1	97.0	97.2
HSS	0.274	0.242	0.172	0.639	0.626	0.639
POD	0.195	0.153	0.110	0.602	0.586	0.591
FAR	0.425	0.250	0.435	0.283	0.292	0.269
CSI	0.170	0.145	0.102	0.486	0.472	0.486

5.2 Wind Speed Frequency Distributions. The model (A) proposed by Det 21 shows some skill using the dependent dataset, but any of the models containing MAXWND do almost twice as well. The percent correct by 10-knot categories increases from 47 to 65 when MAXWND is added. There are no major differences in skill between the three models that contain only pressure gradient information. Table 9 gives the frequency of winds (by 10-knot categories) that occur when both pressure gradients are greater than 4 mb. Compare Table 9 with Table 10, which gives the frequency of northwest winds greater than 10 knots when both pressure gradients are less than 4 mb. As the tables show, 20 percent of northwest winds greater than 40 knots occur when at least one pressure gradient is less than 4 mb. These cases were not included in the regression. The frequency distribution of MAXPDDIR is shown in Table 11. The wind direction is usually between 240 and 330 degrees, with a peak at 300.

TABLE 9. Wind Speed Frequency Distribution--Both Pressure Gradients Greater than 4 mb (Dependent Data Set).

Wind Speed	Frequency	Cumulative Percent	Cumulative Frequency	Percent
0- 9	94	3.6	94	3.6
10-19	832	32.3	926	35.9
20-29	983	38.1	1909	74.0
30-39	554	21.4	2463	95.4
40-49	99	3.9	2562	99.3
50-59	18	0.7	2580	100.0
60-69	1	0.0	2581	100.0

TABLE 10. Wind Speed Frequency Distribution--At Least One Pressure Gradient Less than 4 mb, Direction Between 270 and 360°, Speed Greater than 10 kts (Dependent Data Set).

Wind Speed	Frequency	Cumulative Percent	Cumulative Frequency	Percent
10-19	1508	55.7	1508	55.7
20-29	763	34.0	2426	89.7
30-39	258	9.5	2684	99.2
40-49	22	0.7	2706	100.0

TABLE 11. Wind Direction Frequency Distribution--Both Pressure Gradients Greater than 4 mb (Dependent Data Set).

Wind Direction	Frequency	Cumulative Percent	Cumulative Frequency	Percent
0-29	0	0.0	0	0.0
30-59	1	0.0	1	0.0
60-89	0	0.0	1	0.0
90-119	0	0.0	1	0.0
120-149	0	0.0	1	0.0
150-179	0	0.0	1	0.0
180-209	0	0.0	1	0.0
210-239	57	2.2	58	2.2
240-269	399	15.5	457	17.7
270-299	792	30.7	1249	48.4
300-329	1175	45.5	2424	93.9
330-360	157	6.1	2581	100.0

5.3 Reducing the Pressure Gradient. Experiments using several different thresholds for the two pressure gradients were run to improve the number of events included in the regression. A gradient of 1 mb was selected because it had the least effect on the skill scores and included all but eight wind events greater than 40 knots. Tables 12 and 13 are the verification matrices for models A and E, respectively.

TABLE 12. Verification Matrix for Candidate Model A--Both Pressure Gradients Greater than 1 mb (Dependent Data Set).

	FORECAST WINDS						
OBSVD WINDS	0-9	10-19	20-29	30-39	40-49	50-59	60-69
0-9	0	721	35	1	0	0	0
10-19	0	1708	568	8	0	1	0
20-29	0	829	838	55	0	0	0
30-39	0	205	405	117	13	1	0
40-49	0	16	48	44	9	4	0
50-59	0	0	4	9	5	0	0
60-69	0	0	0	0	1	0	0

TABLE 13. Verification Matrix for Candidate Model E--Both Pressure Gradients Greater than 1 mb (Dependent Data Set).

OBSVD WINDS	FORECAST WINDS 0-9	10-19	20-29	30-39	40-49	50-59	60-69
0-9	306	450	1	0	0	0	0
10-19	119	1911	250	0	0	0	0
20-29	11	581	1018	107	0	0	0
30-39	0	67	267	370	35	0	0
40-49	0	4	16	42	54	4	0
50-59	0	1	0	0	6	10	0
60-69	0	0	0	0	0	0	1

TABLE 14. Verification Statistics for Candidate Models Using Surface Observations--Both Pressure Gradients Greater than 1 mb (Dependent Data Set).

Model	A	B	C	D	E	F
R^2	0.357	0.253	0.298	0.722	0.737	0.745
Ten knots						
Percent Correct	47	45	47	65	65	66
HSS	0.306	0.245	0.280	0.620	0.619	0.628
Weather Warning						
Percent Correct	97.6	97.6	97.6	97.1	98.2	97.2
HSS	0.211	0.114	0.135	0.639	0.594	0.615
POD	0.136	0.064	0.077	0.602	0.544	0.562
FAR	0.441	0.308	0.353	0.283	0.324	0.300
CSI	0.123	0.063	0.075	0.486	0.431	0.453

5.4 The Advantages of a New Threshold. The coefficient of determination increased for all models, while the HSS varied slightly. The skill of the models that used only the pressure gradients dropped more consistently than the other models. The advantage of this new threshold can be seen in Tables 15 and 16. The number of high-wind cases that were considered was increased. The wind direction is still predominately from the northwest with a peak at 300°-see Table 16. The range of wind directions is slightly larger with this criteria.

TABLE 15. Wind Speed Frequency Distribution--Both Pressure Gradients Greater than 1 mb (Dependent Data Set).

Wind Speed	Frequency	Percent	Cumulative Frequency	Cumulative Percent
0- 9	757	13.4	757	13.4
10-19	2285	40.5	3042	53.9
20-29	1722	30.5	4764	84.4
30-39	741	13.1	5505	97.5
40-49	121	0.4	5626	99.7
50-59	18	0.3	5644	100.0
60-69	1	0.0	2645	100.0

TABLE 16. Wind Speed Frequency Distribution--At Least One Pressure Gradient Less Than 1 mb, Direction Between 270 and 360°, Speed Greater Than 10 Knots (Dependent Data Sets).

Wind Speed	Frequency	Percent	Cumulative Frequency	Cumulative Percent
10-19	921	64.3	921	64.3
20-29	387	27.0	1308	91.3
30-39	117	8.1	1425	99.4
40-49	8	0.6	1433	100.0

TABLE 17. Wind Direction Frequency Distribution--Both Pressure Gradients Greater than 1 mb (Dependent Data Set).

Wind Direction	Frequency	Percent	Cumulative Frequency	Cumulative Percent
0-29	8	0.1	8	0.1
30-59	1	0.0	9	0.2
60-89	0	0.0	9	0.2
90-119	0	0.0	9	0.2
120-149	1	0.0	10	0.2
150-179	2	0.0	12	0.2
180-209	43	0.8	55	1.0
210-239	312	5.5	367	6.5
240-269	949	16.8	1316	23.3
270-299	1372	24.3	2688	47.6
300-329	2365	41.9	5053	89.5
330-360	592	10.5	5645	100.0

5.5 Inflation Applied. Since the candidate models were not forecasting all weather warning events, inflation was used. As mentioned earlier, inflation increases wind forecasts above the mean and decreases them below the mean. Verification matrices for Models A and E, using inflation with the 1-mb threshold on the pressure gradients, are given in Tables 18 and 19. The HSS (when the data is grouped by 10-knot increments) increases in all cases, but the increase is larger with the models that only use pressure gradients. The HSS for weather warning verification decreases due to the larger number of false alarms. The POD increases by 0.10, but the FAR almost doubles in most cases.

TABLE 18. **Verification Matrix for Candidate Model A--Both Pressure Gradients Greater than 1 mb, Inflation Used (Dependent Data Set).**

OBSVD WINDS	FORECAST WINDS 0-9	10-19	20-29	30-39	40-49	50-59	60-69
0-9	353	364	39	0	0	1	0
10-19	408	1261	531	79	4	1	1
20-29	151	628	632	272	37	2	0
30-39	32	160	232	205	81	25	6
40-49	0	15	26	32	29	9	10
50-59	0	0	3	1	4	9	1
60-69	0	0	0	0	0	0	1

TABLE 19. **Verification Matrix for Candidate Model E--Both Pressure Gradients Greater than 1 mb, Inflation Used (Dependent Data Set).**

OBSVD WINDS	FORECAST WINDS 0-9	10-19	20-29	30-39	40-49	50-59	60-69
0-9	486	270	1	0	0	0	0
10-19	243	1780	257	0	1	0	0
20-29	22	565	921	209	0	0	0
30-39	0	65	192	392	89	1	0
40-49	0	4	11	30	59	15	1
50-59	0	1	0	0	5	7	4
60-69	0	0	0	0	0	0	1

TABLE 20. Verification Statistics for Candidate Models Using Surface Observations--Both Pressure Gradients Greater than 1 mb, Inflation Used (Dependent Data Set).

Model	A	B	C	D	E	F
Ten knots						
Percent Correct	44	39	45	64	65	64
HSS	0.376	0.284	0.338	0.636	0.643	0.639
Weather Warning						
Percent Correct	95.8	96.2	96.7	97.4	97.6	97.5
HSS	0.329	0.319	0.297	0.537	0.561	0.550
POD	0.450	0.393	0.300	0.643	0.667	0.657
FAR	0.715	0.703	0.672	0.519	0.497	0.508
CSI	0.211	0.204	0.186	0.380	0.402	0.391

5.6 Independent Verification. Data for 1987 through 1989 was saved for independent verification of the models. The verification matrices for models A and E are given in Tables 21 and 22. As would be expected, the skill scores decrease on the independent data set, as shown in Table 23. None of the models using only pressure gradients forecast weather warning criteria winds greater than 40 knots. Table 24 shows the frequency distribution of the wind speed. Almost as many weather warning winds were not forecast using the 1-mb criteria in 1987 through 1989 as were missed in the entire dependent data set (six compared to eight--see Table 25). The frequency distribution of wind direction is almost identical to the dependent data set--see Table 26.

TABLE 21. Verification Matrix for Candidate Model A--Both Pressure Gradients Greater than 1 mb (Independent Data Set).

OBSVD WINDS	FORECAST WINDS 0-9	10-19	20-29	30-39	40-49	50-59	60-69
0-9	0	154	10	0	0	0	0
10-19	0	444	224	6	0	0	0
20-29	0	154	169	10	0	0	0
30-39	0	43	104	35	0	0	0
40-49	0	2	7	3	0	0	0
50-59	0	0	0	0	0	0	0
60-69	0	0	0	0	0	0	0

TABLE 22. Verification Matrix for Candidate Model E--Both Pressure Gradients Greater than 1 mb (Independent Data Set).

OBSVD WINDS	FORECAST WINDS 0-9	10-19	20-29	30-39	40-49	50-59	60-69
0-9	56	108	0	0	0	0	0
10-19	21	533	119	0	0	0	0
20-29	2	118	189	24	0	0	0
30-39	1	14	64	97	5	0	0
40-49	0	0	1	8	3	0	0
50-59	0	0	0	0	0	0	0
60-69	0	0	0	0	0	0	0

TABLE 23. Verification Statistics for Candidate Models using Surface Observations--Both Pressure Gradients Greater than 1 mb (Independent Data Set).

Model	A	B	C	D	E	F
Ten knots						
Percent Correct	47	44	47	64	64	53
HSS	0.261	0.190	0.261	0.566	0.572	0.467
Weather Warning						
Percent Correct	99.1	99.1	99.1	99.0	98.9	97.8
HSS	0.000	0.000	0.000	0.218	0.295	0.277
POD	0.000	0.000	0.000	0.167	0.250	0.546
FAR	0.000	0.000	0.000	0.667	0.625	0.807
CSI	0.000	0.000	0.000	0.125	0.176	0.167

TABLE 24. Wind Speed Frequency Distribution--Both Pressure Gradients Greater than 1 mb (Independent Data Set).

Wind Speed	Frequency	Percent	Cumulative Frequency	Cumulative Percent
0- 9	164	12.0	164	12.0
10-19	674	49.4	838	61.4
20-29	333	24.4	1171	85.8
30-39	182	13.3	1353	99.1
40-49	12	0.9	1365	100.0

TABLE 25. Wind Speed Frequency Distribution--at Least One Pressure Gradient Less than 1 mb, Direction Between 270 and 360°, Speed Greater than 10 Knots. (Independent Data Set).

Wind Speed	Frequency	Percent	Cumulative Frequency	Cumulative Percent
10-19	203	66.8	203	66.8
20-29	75	24.6	278	91.4
30-39	20	6.6	298	98.0
40-49	6	2.0	304	100.0

TABLE 26. Wind Direction Frequency Distribution--Both Pressure Gradients Greater than 1 mb (Independent Data Set).

Wind Direction	Frequency	Percent	Cumulative Frequency	Cumulative Percent
0-29	4	0.3	4	0.3
30-59	0	0.0	4	0.3
60-89	0	0.0	4	0.3
90-119	0	0.0	4	0.3
120-149	1	0.1	5	0.4
150-179	0	0.0	5	0.4
180-209	13	0.9	18	1.3
210-239	72	5.3	90	6.6
240-269	231	16.9	321	23.5
270-299	329	24.1	650	47.6
300-329	565	41.4	1215	89.0
330-360	150	11.0	1365	100.0

TABLE 27. Verification Matrix for Candidate Model A--Both Pressure Gradients Greater than 1 mb, Inflation Used (Independent Data Set).

OBSVD WINDS	FORECAST WINDS 0-9	10-19	20-29	30-39	40-49	50-59	60-69
0-9	67	85	12	0	0	0	0
10-19	66	351	223	32	2	0	0
20-29	13	139	118	60	3	0	0
30-39	5	37	51	67	20	2	0
40-49	0	2	2	6	2	0	0
50-59	0	0	0	0	0	0	0
60-69	0	0	0	0	0	0	0

TABLE 28. Verification Matrix for Candidate Model E--Both Pressure Gradients Greater than 1 mb, Inflation Used (Independent Data Set).

OBSVD WINDS	FORECAST WINDS 0-9	10-19	20-29	30-39	40-49	50-59	60-69
0-9	84	80	0	0	0	0	0
10-19	51	497	124	1	0	0	0
20-29	2	118	177	36	0	0	0
30-39	3	12	57	85	24	0	0
40-49	0	0	0	0	6	5	1
50-59	0	0	0	0	0	0	0
60-69	0	0	0	0	0	0	0

TABLE 29. Verification Statistics for Candidate Models using Surface Observations--Both Pressure Gradients Greater than 1 mb, Inflation Used (Independent Data Set).

Model	A	B	C	D	E	F
Ten knots						
Percent Correct	44	39	44	62	62	50
HSS	0.333	0.249	0.333	0.578	0.576	0.468
Weather Warning						
Percent Correct	97.3	99.1	97.3	97.7	97.8	97.8
HSS	0.086	0.116	0.086	0.195	0.277	0.183
POD	0.167	0.250	0.167	0.333	0.500	0.636
FAR	0.931	0.914	0.931	0.852	0.800	0.885
CSI	0.051	0.068	0.051	0.114	0.167	0.108

5.7 Summary of Results. The use of inflation resulted in better HSSs for all models in the independent data set. The three models that used only the pressure gradient predicted some weather warning events even though the POD remained low. The three models that contain MAXWND selected from one- to two-thirds of the weather warning events. The FAR for all these models remained high. Model E showed the best skill on the independent dataset. Even though the POD was a little lower than Model F, the FAR was better. Based on the dependent data set, model D showed promise, but it forecast two fewer weather warning wind cases than model E in the independent data set. None of the models using only pressure gradient had a POD significantly high enough to use in weather warning forecasting.

5.8 Lead Times. Det 21 asked for an estimated elapsed time after the 4-mb pressure gradient threshold was passed before winds greater than 40 knots would occur. When pressure gradients are greater than 4 mb, wind speed is usually less than 40 knots; therefore, only lead time for wind forecasts over 40 knots was calculated. If the previous 3-hour forecast indicated winds over 40 knots, a lead time was not included in the average. In the dependent data set, 29 events were used in the average. The average lead time was 119 minutes. Five weather warnings did not have lead times. In the independent data set, average lead time was 160 minutes.

5.9 Refinement: Adding 700-mb Winds. Det 21 also asked that the 700-mb wind be related to the FCSTMAX over a 12-hour period when wind speed was greater than 30 knots. Table 30 is the dependent data set verification; it shows that R^2 is never above 0.25 and that upper-air variables account for less than 25 percent of the variability. When just the 700- or 850-mb winds are used, no winds greater than 40 knots were predicted. When inflation was applied (Table 31), skill improved, but the actual forecast values became erratic due to the low values of R. Inflation results in a better POD comparable to the surface observations, but the FAR is higher than the surface observations.

TABLE 30. Verification Statistics for Candidate Models Using Upper-Air Observations--Winds Greater Than 30 kts (Dependent Data Set).

Model	U	V	W	X	Y	Z
R^2						
00 UTC	0.100	0.072	0.167	0.189	0.220	
12 UTC	0.086	0.046	0.252	0.250	0.210	
Ten knots						
Percent Correct	37	34	41	40	40	
HSS	0.094	0.019	0.205	0.224	0.210	
Weather Warning						
Percent Correct	96.7	93.5	96.7	93.5	92.2	
HSS	0.000	0.000	0.033	0.035	0.031	
POD	0.000	0.000	0.018	0.019	0.021	
FAR	0.000	0.000	0.000	0.000	0.667	
CSI	0.000	0.000	0.018	0.019	0.020	

TABLE 31. Verification Statistics for Candidate Models Using Upper-Air Observations--Winds Greater than 30 kts, Inflation Used (Dependent Data Set).

Model	U	V	W	X	Y	Z
Ten knots						
Percent Correct	28	28	29	28	26	
HSS	0.130	0.198	0.220	0.198	0.176	
Weather Warning						
Percent Correct	84.1	77.5	84.5	77.5	74.2	
HSS	0.127	0.195	0.169	0.195	0.225	
POD	0.509	0.660	0.632	0.660	0.766	
FAR	0.895	0.823	0.871	0.823	0.804	
CSI	0.096	0.162	0.120	0.162	0.185	

5.10 Independent Verification--Upper-Air. Independent verification showed almost no skill when using upper-air observations, with or without inflation. Even though inflation improved the POD, there were almost 20 times more false alarms than correct forecasts. None of the models showed a statistically significant distribution different from randomness as measured by a Chi Square test.

TABLE 32. Verification Statistics for Candidate Models using Upper-Air Observations--Winds Greater than 30 kts (Independent Data Set).

Model	U	V	W	X	Y
Ten knots					
Percent Correct	38	24	42	29	3
HSS	0.141	0.037	0.224	0.123	0.000
Weather Warning					
Percent Correct	97.9	96.7	97.9	96.6	5.5
HSS	0.000	0.000	0.000	0.000	0.001
POD	0.000	0.000	0.000	0.000	1.000
FAR	0.000	0.000	0.000	0.000	0.965
CSI	0.000	0.000	0.000	0.000	0.021

TABLE 33. Verification Statistics for Candidate Models Using Upper-Air Observations--Winds Greater than 30 kts, Inflation Used (Independent Data Set).

Model	U	V	W	X	Y
Ten knots					
Percent Correct	24	5	33	20	0
HSS	0.121	0.004	0.249	0.101	-0.052
Weather Warning					
Percent Correct	86.3	22.7	89.7	70.3	3.4
HSS	0.059	0.016	0.031	0.024	0.000
POD	0.333	1.000	0.167	0.400	0.000
FAR	0.946	0.960	0.960	0.954	0.000
CSI	0.049	0.041	0.031	0.043	0.000

6. DISCUSSION.

6.1 Limitations. Local pressure gradients and surface variables at Minot AFB were used in developing a method for forecasting gusty winds for that station. The study showed that even the best of models will not provide 100 percent accuracy in issuing weather warnings or TAFs. The best explanation for this is shown in Figure 3; even though a straight line can be drawn through the data, the data spread is so great that forecasting a specific threshold such as 40 knots would result in large errors. For Model E, the 5th and 95th percent confidence intervals (the lower and upper intervals, respectively) that produce a correct forecast 90 percent of the time, are plus or minus 10 knots. Models A, B and C have a confidence interval closer to plus or minus 15 knots.

6.2 Persistence. Winds, like most other weather elements, are persistent, and persistence accounts for the high correlation between the current wind and the maximum wind over the next 6 hours. A persistence forecast in the dependent data set results in a HSS of 0.551 for 10-knot intervals and 0.587 for weather warning criteria. Persistence is better than those surface models with only pressure gradients. The other three surface models showed skill compared to persistence. Although persistence forecast 59 weather warning events, winds greater than 40 knots were already occurring. Model E forecast the start of 33 events, something persistence cannot do. Models D, E, and F also beat persistence on the independent data set, where persistence had an HSS of 0.495 for the 10-knot category and 0.153 for the weather warning verification.

6.3 MOS Forecasting. Another statistical method of forecasting surface winds is MOS, which combines surface observations with variables taken from the LFM model to produce a wind forecast valid every 6 hours. MOS does not forecast gusts. Capt David Miller, the AWS Liaison Officer to the Technique Development Laboratory (TDL), provided MOS verification for Minot AFB, ND. Six-hour MOS forecasts of northwest winds (270-360) at 00 and 12Z from 1 October 1985 until 31 March 1990 had HSSs of 0.538 and 0.534, respectively. These forecasts were verified for winds between from 0 and 15, 16 and 25, and greater than 25 knots. Even though the forecast is for wind speed and verified for slightly different thresholds, its quality is comparable to that of Model E, which was produced by this study. TDL tried to develop a MOS product to predict wind gusts, but it did not verify any better than multiplying the MOS forecast wind speed by 1.5 (Carter and Dagostoro, 1985).

6.4 Geostrophic Wind Forecasting. AWSP 105-56, *Meteorological Techniques*, includes an approved geostrophic wind forecast technique (Boehm, 1979) that suggests forecasting 2/3 of the geostrophic wind during the time of maximum mixing, and forecasting a surface wind direction 40 degrees less than the geostrophic direction. The geostrophic wind is forecast by using the geostrophic wind chart, a facsimile product transmitted every 3 hours. Unfortunately, the geostrophic wind information is not archived and statistics cannot be presented; however, forecasters at Kelly AFB have found that the geostrophic wind chart works well there. The technique allows a representative wind for the air mass that will be influencing the weather to be selected; e.g., a value north of the cold front after frontal passage.

6.5 The Recommended Model. Model E is an acceptable objective method for identifying synoptic situations that might produce strong gusty winds. A perfect method of forecasting weather warning criteria may never be found, but an evaluation of the synoptic situation, in conjunction with this objective method (Model E) should improve the forecast. Several factors cannot readily be included in an objective technique. When the pressure gradient is measured across 250 NM, the gradient near the center can be significantly different than the gradient overall. The strength of the inversion and, more importantly, if and when it may dissipate, can also be a key to forecasting the peak wind when the upper-level winds are strong. No objective method for determining surface temperature late in the 12-hour period is available. Factors such as whether or not the ground is snow-covered, cloud cover amount, and temperature advection all play an important part in forecasting temperature change.

7. CONCLUSIONS.

7.1 The Study Summarized. Surface and upper-air variables were evaluated for use in forecasting strong northwesterly winds at the surface. The best correlation with the maximum wind speed during the next 6 hours is with the current maximum wind speed. With the addition of the pressure gradient between Glasgow, MT, and Yorkton, Canada, and the Minot sea level pressure, an effective method of forecasting gusty winds is achieved with USAFETAC's Model E. For this method to be valid, pressure gradients between Dickinson, ND, and Portage La Prairie, Canada, and between Glasgow, MT, and Yorkton, Canada, must be greater than 1 mb. The HSS is 0.572 on the independent data when grouped into 10-knot categories. The Model E score is better than persistence and slightly better than MOS skill. Weather warning verification using the independent data shows this technique to perform worse than the current forecasters. A wind direction of 300 degrees should be used with this method.

7.2 Inflation Recommended. Inflation increases the wind forecast when the objective wind forecast is above the dependent data mean. This increases the number of weather warnings correctly forecast, but also increases the number of false alarms. For model E, the POD increased from 0.25 to 0.50, but the FAR also increased from 0.63 to 0.80. Inflation should be used with this algorithm.

7.3 Upper-Air Data Not Recommended. None of the models using upper-air data produced a method for forecasting gusty surface winds. Skill scores were low, and most of the forecast distributions were not significantly different from chance.

7.4 Model "E" Recommended. None of the models in this report can be used successfully in isolation, but Model E, in conjunction with analysis of the synoptic situation, should improve Minot's current wind forecasting capability from October through March.

REFERENCES

Boehm, A., "Geostrophic Wind and Its Use For Surface Wind Forecasts," AWSP 105-56, *Meteorological Techniques*, HQ Air Weather Service, Scott AFB, IL, April 1982.

Carter, Gary M., and Valery J. Dagostaro, *Testing MOS Surface Wind Gust Prediction Equations*, TDL Office Note 85-6, Techniques Development Laboratory, Washington, DC, March 1985.

Duffield, George F., and Gregory Nastrom, *Equations and Algorithms for Meteorological Applications in Air Weather Service*, AWS/TR-83/001, HQ Air Weather Service, Scott AFB, IL, December 1983.

Goldsmith, Barry S., *A Comprehensive Analysis of Verification Results for Forecasts of Precipitation Type and Snow Amount*, Preprint, 11th Conference on Probability and Statistics in Atmospheric Science, Monterey, CA, October, 1989.

Klein, W.H., B.M. Lewis, and I. Enger, "Objective Prediction of Five-Day Mean Temperatures during Winter," *J. Meteorol*, vol 16, pp 672-682.

Ott, Lyman, *An Introduction to Statistical Methods and Data Analysis*, PWS-KENT Publishing Company, Boston, MA, 1988.

Some Techniques for Deriving Objective Forecasting Aids and Methods, AWS TR 235, HQ Air Weather Service, Scott AFB, IL, April 1955.

SPECIALIZED TERMS AND ACRINABs

ACRINAB	acronym, initialism, or abbreviation
BWS	Base Weather Station
CSI	Critical Skill Index
DELP24	24-hour change in sea level pressure (mb)
DELT24	24-hour change in temperature (C)
DIK	Station identifier for Dickinson, ND
DIKMYPG	Pressure gradient between Dickinson, ND and Portage la Prairie, Canada (mb)
DIR1070	Direction of the shear vector between the surface and 700 mb (kts)
DIR1085	Direction of the shear vector between the surface and 850 mb (kts)
DIR500	500 mb wind direction in degrees
DIR700	700 mb wind direction in degrees
DIR850	850 mb wind direction in degrees
f	Coriolis parameter
FAR	False Alarm Rate
FCSTMAX	Objective forecast of the maximum wind (kts)
GGW	Station identifier for Glasgow, MT
GGWMYQV	Pressure gradient between Glasgow, MT and Yorkton, Canada (mb)
HRDUM	Dummy time variable set to 1 between 21 and 9 UTC; otherwise, it is 0.
HSS	Heidke Skill Score
INVDEPTH	Depth of the first inversion above the surface and below 700 mb.
MAXPDDIR	Wind direction for MAXPDWND.

MAXPDWND	Maximum wind reported during the period (6 or 12 hours) (kts)
MAXWND	Maximum wind either speed or gust reported on an observation (kts)
MOS	Model Output Statistics
n	Axis perpendicular to the wind.
NWS	National Weather Service
p	pressure
POD	Probability of Detection
R	Pearson Product-Moment Correlation Coefficient
R^2	coefficient of determination
SLP	Sea Level Pressure (mb)
SPD1070	Magnitude of the shear vector between the surface and 700 mb (kts)
SPD1085	Magnitude of the shear vector between the surface and 850 mb (kts)
STABLE	Difference between the temperature at 850 mb and the surface temperature.
STRENGTH	Gradient of temperature across the inversion C/m.
TEMP	Surface temperature (C)
TEMP50	500 mb temperature (C)
TEMP70	700 mb temperature (C)
TEMP85	850 mb temperature (C)
TIMELAG	Number of minutes between the start of the period and the maximum wind.
UCOMP50	u-component (E-W) of the 500 mb wind speed (kts)
UCOMP70	u-component (E-W) of the 700 mb wind speed (kts)
UCOMP85	u-component (E-W) of the 850 mb wind speed (kts)

UDIRBAR	Mean u-component of the wind for a 6 or 12 hour period (kts)
VCOMP50	v-component (N-S) of the 500 mb wind speed (kts)
VCOMP70	v-component (N-S) of the 700 mb wind speed (kts)
VCOMP85	v-component (N-S) of the 850 mb wind speed (kts)
VDIRBAR	Mean v-component of the wind for a 6 or 12 hour period (kts)
WND500	500 mb wind speed (kts)
WND700	700 mb wind speed (kts)
WND850	850 mb wind speed (kts)
YQV	Station identifier for Yorkton, Canada
YPG	Station identifier for Portage la Prairie, Canada

DISTRIBUTION

AWS/DO, Scott AFB, IL 62225-5008 2
AWS/XT, Scott AFB, IL 62225-5008 2
OL A, HQ AWS, Buckley ANG Base, Aurora, CO 80011-9599 1
SD/CWDA, PO Box 92960, Los Angeles, CA 90009-2960 1
OL-K, HQ AWS, NEXRAD Opnl Support Facility, 1200 Westheimer Dr. Norman, OK 73069 1
OL-M, HQ AWS, McClellan AFB, CA 95652-5609 1
Det 1, HQ AWS, Pentagon, Washington, DC 20330-6560 3
Det 2, HQ AWS, Pentagon, Washington, DC 20330-5054 3
Det 3, HQ AWS, PO Box 3430, Onizuka AFB, CA 94088-3430 1
Det 9, HQ AWS, PO Box 12297, Las Vegas, NV 89112-0297 1
1WW/DN, Hickam AFB, HI 96853-5000 3
    11WS/DON, Elmendorf AFB, AK 99506-5000 1
    20WS/DON, APO San Francisco 96328-5000 1
    30WS/DON, APO San Francisco 96301-0420 1
2WW/DN, APO New York 09094-5000 3
    7WS/DON, APO New York 09403-5000 1
    28WS/DON, APO New York 09127-5000 1
    31WS/DON, APO New York 09136-5000 1
3WW/DN, Offutt AFB, NE 68113-5000 6
    9WS/DON, March AFB, CA 92518-5000 10
    Det 21, 9WS, Minot AFB, ND 58705-5000 5
    24WS/DON, Randolph AFB, TX 78150-5000 1
    26WS/DON, Barksdale AFB, LA 71110-5002 1
4WW/DN, Peterson AFB, CO 80914-5000 3
    2WS/DON, Andrews AFB, MD 20334-5000 20
5WW/DN, Langley AFB, VA 23665-5000 3
    1WS/DON, MacDill AFB, FL 33608-5000 1
    3WS/DON, Shaw AFB, SC 29152-5000 1
    5WS/DON, Ft McPherson, GA 30330-5000 1
    25WS/DON, Bergstrom AFB, TX 78743-5000 1
AFGWC/SDSL, Offutt AFB, NE 68113-5000 3
    USAFETAC, Scott AFB, IL 62225-5438 6
7WW/DN, Scott AFB, IL 62225-5008 3
    6WS/DON, Hurlburt Field, FL 32544-5000 1
    15WS/DON, McGuire AFB, NJ 08641-5002 1
    17WS/DON, Travis AFB, CA 94535-5986 1
3350 TCHTG/TTGU-W, Stop 62, Chanute AFB, IL 61868-5000 2
3395 TCHTG/TTKO, Keesler AFB, MS 39534-5000 2
AFIT/CIR, Wright-Patterson AFB, OH 45433-6583 1
AFCSA/SAGW, Washington, DC 20330-5000 1
NAVOCEANCOMDET, Federal Building, Asheville, NC 28801-2723 1
NAVOCEANCOMDET, Patuxent River NAS, MD 20670-5103 1
NAVOCEANCOMFAC, Stennis Space Ctr, MS 39529-5002 1
NAVOCEANCOMFAC, NAS North Island, San Diego, CA 92135-5130 1
COMNAVOCEANCOM, Code N312, Stennis Space Ctr, MS 39529-5000 1
NAVOCEANO, Code 9220 (Tony Ortolano),Stennis Space Ctr, MS 39529-5001 1
Maury Oceanographic Library (NOC), Code XJL, Stennis Space Ctr, MS 39529-5001 1
FLENUMOCEANCEN, Monterey, CA 93943-5006 1
NOARL West, Monterey, CA 93943-5006 1
Naval Research Laboratory, Code 4323, Washington, DC 20375 1

Naval Postgraduate School, Chmn, Dept of Meteorology, Code 63, Monterey, CA 93943-5000 1
Naval Eastern Oceanography Ctr, U117 McCAdy Bldg, NAS Norfolk, Norfolk, VA 23511-5000 1
Naval Western Oceanography Ctr, Box 113, Attn: Tech Library, Pearl Harbor, HI 96860-5000 1
Naval Oceanography Command Ctr, COMNAVMAR Box 12, FPO San Francisco, CA 96630-5000 1
Pacific Missile Test Center, Geophysics Division, Code 3253, Pt Mugu, CA 93042-5000 1
Dept of Commerce/NOAA/MASC, Library MC5 (Jean Bankhead), 325 Broadway, Boulder, CO 80303 2
OFCM, Suite 900, 6010 Executive Blvd, Rockville, MD 20852 1
NOAA Library-EOC4WSC4, Attn: ACQ, 6009 Executive Blvd, Rockville, MD 20852 1
NOAA/NESDIS (Attn: Nancy Everson, E/RA22), World Weather Bldg, Rm 703, Washington, DC 20233 1
NOAA/NESDIS (Attn: Capt Taylor), FB #4, Rm 0308, Suitland, MD 20746 1
Armed Forces Medical Intelligence Agency, Info Svcs Div., Bldg 1607, Ft Detrick, Frederick, MD 21701-5004 1
GL/LY, Hanscom AFB, MA 01731-5000 1
GL Library, Attn: SULLR, Stop 29, Hanscom AFB, MA 01731-5000 1
Atmospheric Sciences Laboratory, Attn: SLCAS-AT-AB, Aberdeen Proving Grounds, MD 21005-5001 1
Atmospheric Sciences Laboratory, White Sands Missile Range, NM 88002-5501 1
U.S. Army Missile Command, ATTN: AMSMI-RD-TE-F, Redstone Arsenal, AL 35898-5250 1
Commander and Director, U.S. Army CEETL, Attn: GL-AE, Fort Belvoir, VA 22060-5546 1
Technical Library, Dugway Proving Ground, Dugway, UT 84022-5000 1
NWS W/OSD, Bldg SSM C-2, East-West Hwy, Silver Spring, MD 20910 1
NWS Training Center, 617 Hardesty, Kansas City, MO 64124 1
NCDC Library (D542X2), Federal Building, Asheville, NC 28801-2723 1
NIST Pubs Production, Rm A-405, Admin Bldg, Gaithersburg, MD 20899 1
JSOC/Weather, P.O. Box 70239, Fort Bragg, NC 28307-5000 1
75th RGR (Attn: SWO), Ft Benning, GA 31905-5000 1
DTIC-FDAC, Cameron Station, Alexandria, VA 22304-6145 2
AUL/LSE, Maxwell AFB, AL 36112-5564 1
AWSTL, Scott AFB, IL 62225-5438 35